



Contents lists available at ScienceDirect

Bioorganic & Medicinal Chemistry Letters

journal homepage: www.elsevier.com/locate/bmcl

Non-oxime pyrazole based inhibitors of B-Raf kinase

Bradley J. Newhouse^{a,*}, Joshua D. Hansen^a, Jonas Grina^a, Mike Welch^a, George Topalov^a, Nicole Littman^a, Michele Callejo^a, Matthew Martinson^a, Sarah Galbraith^a, Ellen R. Laird^a, Barbara J. Brandhuber^a, Guy Vigers^a, Tony Morales^a, Rich Woessner^a, Nikole Randolph^a, Joseph Lyssikatos^b, Alan Olivero^b

^a Array BioPharma, 3200 Walnut Street, Boulder, CO 80301, United States

^b Genentech, Inc., 1 DNA Way, South San Francisco, CA 94080-4990, United States

ARTICLE INFO

Article history:

Received 21 October 2010

Revised 2 December 2010

Accepted 6 December 2010

Available online 17 December 2010

Keywords:

B-Raf

Oxime

Pyrazole

ABSTRACT

The synthesis and biological evaluation of non-oxime pyrazole based B-Raf inhibitors is reported. Several oxime replacements have been prepared and have shown excellent enzyme activity. Further optimization of fused pyrazole **2a** led to compound **38**, a selective and potent B-Raf inhibitor.

© 2010 Elsevier Ltd. All rights reserved.

Raf kinases, part of the mitogen-activated protein kinase pathway (MAPK), exist in three isoforms, A-Raf, B-Raf, and C-Raf (Raf-1), have been shown to be critical for mediating cell proliferation and survival.¹ The Ras-Raf-MEK-ERK pathway has been implicated in up to 30% of human cancers. Much focus has been centered around the serine/threonine kinase B-Raf, which is mutated in 7% of human cancers. Activating mutations in Raf have been observed in melanoma (50–70%), thyroid cancers (40–70%), and ovarian cancer (35%).² The most frequent mutation in B-Raf is the valine for glutamic acid substitution (V600E), which is found in the activation segment of the B-Raf kinase domain.³ This accounts for a 500-fold increase in the basal rate of MEK phosphorylation over wild-type B-Raf, essentially rendering V600E-B-Raf constitutively active.⁴ This makes B-Raf an attractive target for therapeutic intervention.

Significant effort has been ongoing to develop a potent and selective B-Raf inhibitor. A handful of small molecules that are selective have entered clinical trials, such as PLX-4032, XL-281, and RAF265, with others in preclinical development.⁵ We recently reported on pyrazole based B-Raf inhibitors that incorporate an oxime moiety **1a** (Fig. 1).⁶ The oxime provides both a donor and acceptor to a hydrogen bond network that is crucial to the potency and selectivity of the series (Fig. 2). However, compound **1a** showed degradation to its indane ketone with a half-life of 1.3 hours in a simulated gastric fluid assay. To address the oxime chemical instability and potential metabolic liability,⁷ we sought to identify a suitable compound that retained potency and selectivity.

In our previous Letter,⁶ a small number of modified oximes and oxime replacements were reported. The 2,4-dihydroindeno [1,2-c]pyrazole (herein referred to as the fused pyrazole) in compound **2a** (Fig. 1) showed excellent enzyme potency, encouraging cellular activity, and no degradation in a simulated gastric fluid assay. Although pyrazole **2a** is a potent inhibitor, the matched indane oxime is significantly more active. We determined that the tautomer preference for the pyrazole does favor the desired donor-acceptor arrangement (Fig. 3a), and that the difference most likely arises from less optimal distances for the NH::Glu501 contact (Fig. 3b). Despite the lower activity, the potential for improvements in metabolic stability inspired us to further develop the fused pyrazole, as well as to explore other compounds that might provide a similar hydrogen bonding network.

We began by exploring the properties of the fused pyrazole (Table 1).¹⁰ By removing the methylene bridge in the fused pyrazole **2a**, the pendant pyrazole **3a** showed a 30-fold drop in potency

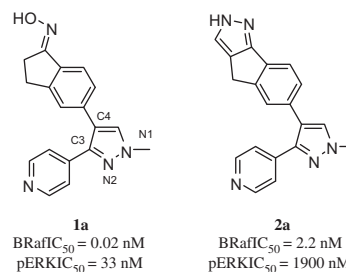


Figure 1. Oxime and non-oxime pyrazole based B-Raf inhibitors.

* Corresponding author.

E-mail address: bnewhouse@arraybiopharma.com (B.J. Newhouse).

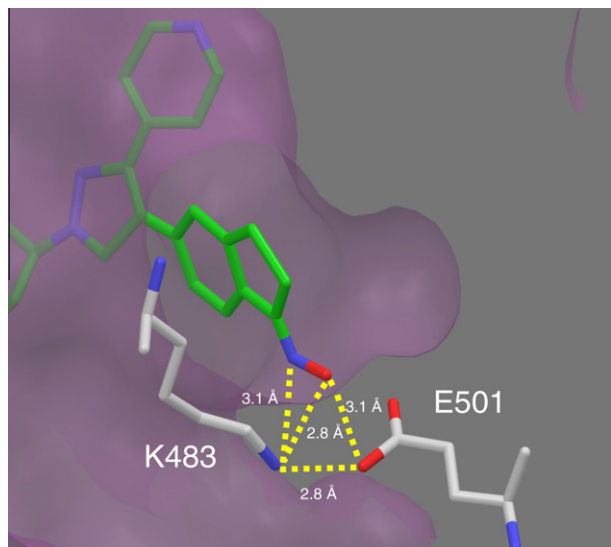


Figure 2. X-ray crystal structure (2.8 Å resolution) of B-Raf in complex with a pyridinyl-pyrazole oxime inhibitor.⁸ The view highlights the hydrogen-bonding network that involves the oxime moiety. The indane ring occupies the largely hydrophobic gatekeeper pocket.

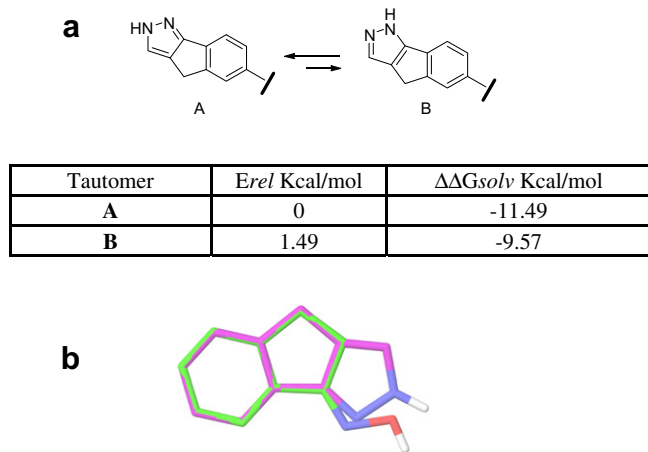


Figure 3. Stereoelectronic comparison of a simplified indane oxime and a fused pyrazole. (a) Relative energies and estimated free energies of solvation for the desired (A) and undesired (B) tautomers of the fused pyrazole suggests that the solution population of A should be dominant.⁹ (b) Comparison of the optimized geometries for the oxime (green) and fused pyrazole (violet) suggests that the ring constraint of the pyrazole prevents close approach of the proton donor to Glu501 if the position of the benzo-fusion is to be retained in its hydrophobic pocket; the oxime hydroxyl also benefits from some rotational flexibility.

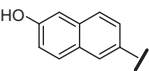
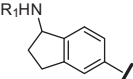
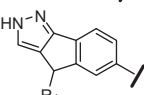
owing to lost hydrophobic contact of the methylene with Ala481 and Thr529.¹¹ Methyl substitution on the pendant pyrazole (**4a**) restored a significant amount of this contact, while ethyl substitution proved sterically excessive (**5a**). Tethering the ethyl group into a six-membered fused pyrazole (**6a**) restored most of the activity; the 10-fold drop in potency versus **2a** is likely caused by residual steric crowding in this very tight space. Repositioning of the donor–acceptor pair from the 4,5-dihydro-2H-benzo[g]indazole **6a** to the 4,5-dihydro-2H-benzo[e]indazole **7a** causes a loss of potency that underscores the requirement for interaction with Lys483 and Glu501. Fused triazole **8a** and pendant triazole **9a** displayed similar behavior to their pyrazole counterparts. When compared to the pendant pyrazole **3a** and triazole **9a**, pyrrole **10a** was 4–14-fold less potent in the enzyme assay, again emphasizing the importance of the hydrogen bond acceptor for Lys483 (Fig. 2).

Table 1
B-Raf enzyme activity of oxime replacements

Compound	R		B-Raf IC ₅₀ (nM)
	a	b	
3a			68
4a			7
5a			>1000
6a			23
7a			>1000
8a			11
9a			55
10a			788
11a			94
12a			647
13a			>1000
14a			139
15a			468
16a			>1000
17a			861
18a			328
19a			1.4

(continued on next page)

Table 1 (continued)

Compound	R	B-Raf IC ₅₀ (nM)
20a		77
21a		1360
22a		157
23a	R ₁ = =O	>1000
24a	NH ₂	>1000
25a	OH	>1000

Attempts to mimic the oxime or fused pyrazole with various fused heterocycles, amides, and sulfonamides met with limited success (**11a–18a**). Lactam **11a** is unable to deliver the hydrogen bond donor near Glu501, while the *trans* amide **12a** is sterically encumbered by Leu527 at the back of the gatekeeper pocket. The fused heterocycles **14a–18a** either lack an acceptor, and/or are unable to position the donor–acceptor pair adequately.

The lipophilic naphthol **19a** was a very potent inhibitor of B-Raf enzyme at 1.4 nM and had excellent cellular activity (pERK IC₅₀ = 78 nM). An X-ray crystal structure of a related series showed that the hydroxyl oxygen superimposes with the center of the oxime N–O bond, hence the hydroxyl is able to act as both donor and acceptor.¹² However, **19a** displayed a high predicted clearance (17 ml/min/kg) in human hepatocytes. The 2-naphthol regioisomer **20a** showed weaker enzyme activity, consistent with its ability to effectively reach only Glu501.

In an attempt to access the Thr529 and Ala481 residues of the gatekeeper pocket, we then investigated substitution at the methylene bridge of the fused pyrazole (compounds **23b–25b**).¹³ Placement of hydrogen bond donors and/or acceptors at this position provided only weak inhibitors. Their weak potency suggested steric crowding, which was later confirmed by crystallography (vide infra).

Because of its promising enzyme and cellular activity, we chose to further optimize compound **2a** by varying the N1 tail of the core pyrazole. The X-ray structure revealed that N1 groups are positioned under the Gly-rich loop and project toward the exit of the ATP cleft.

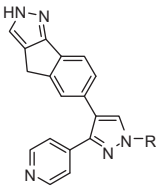
As demonstrated in our earlier report, modifying the N1 position with various solubilizing groups can lead to compounds with excellent enzyme and cell activity. Piperidine substitution at the N1 position provided one of the most potent compounds in the oxime series. This created a sound starting point in the fused pyrazole series (Table 2), such as compound **26** (Fig. 4).

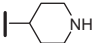
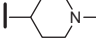
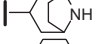
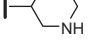
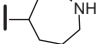
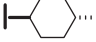
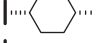
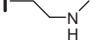
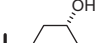
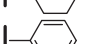
Lipophilic amines **26–32** (Table 2) showed excellent enzyme activity, but varied in cellular potency. *cis*-Amino compound **32** displayed a 35-fold drop in potency relative to its *trans* counterpart **31**. Since the pyrazole core is in an equatorial position on the piperidine ring, the amino group of compound **32** would occupy an axial orientation, placing it closer to the Gly-rich loop of the enzyme.

Removing the conformational restriction of the piperidine ring (**33**) resulted in a 25-fold loss in activity relative to **26**, probably due to loss of surface hydrophobic contacts with the Gly-rich loop. *cis*-Hydroxycyclohexane **34**, whose oxime counterpart is a cell potent compound, proved to be much weaker in the fused pyrazole series. Although aromatic substitution at the N1 position (R = Ph), exemplified by **35**, gave potent enzyme analogs, acceptable cellular activity with these increasingly lipophilic compounds was not obtained.

Table 2

B-Raf enzyme and pERK cell activity of N1 modified pyrazoles with a fused pyrazole head group



Compound	R	B-Raf IC ₅₀ (nM)	pERK IC ₅₀ (nM)	pK _a ^a
26		3	230 (9 nM)	9.80
27		8	886 (10 nM)	8.45
28		0.57	262	10.63
29		3.7	1671	9.31
30		3.2	1540	10.44
31		0.66	396	10.35
32		22.9	1516	10.35
33		72.5	8164	9.56
34		2	607 (7 nM)	
35		4.6	4372	

Numbers in parentheses are from the oxime derivatives.⁶

^a Calculated values of R group nitrogen pK_a's using ACD Labs Release 12.00, Product version 12.00

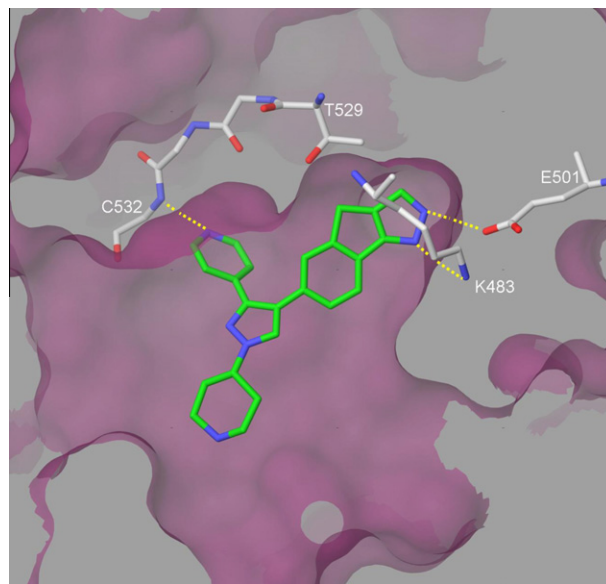
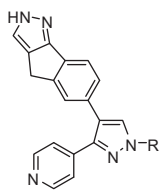


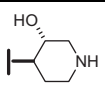
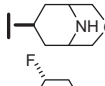
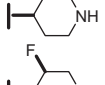
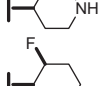
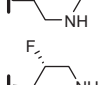
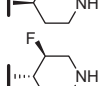
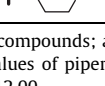
Figure 4. X-ray crystal structure of **26** (3.6 Å resolution) in complex with B-Raf. The view is clipped through the N-terminal lobe with a solvent-accessible surface of the enzyme illustrated in violet; the sidechains of the hinge residues are undisplayed for clarity. Hydrogen bonds are depicted as dashed yellow lines. Coordinates for Compound **26** in B-Raf have been deposited in the PDB, accession code 3PSD.

With the N1 substitution data in hand, we chose to further optimize compound **26**. Although its predicted hepatic clearance was 8 ml/min/kg in human liver microsomes, a concern was its low

Table 3

B-Raf enzyme and pERK cell activity of attenuated piperidine analogs



Compound	R	B-Raf IC ₅₀ (nM)	pERK IC ₅₀ (nM)	pK _a ^b
36		4.9	4871	8.92
37		5	619	8.15
38		1.4	700	7.83
39		3.8	407	
40		3.2	2119	8.18
41^a		1.6	532	
42^a		1.25	672	

^a Enantiopure compounds; absolute stereochemistry not determined.^b Calculated values of piperazine nitrogen pK_a's using ACD Labs Release 12.00, Product version 12.00.

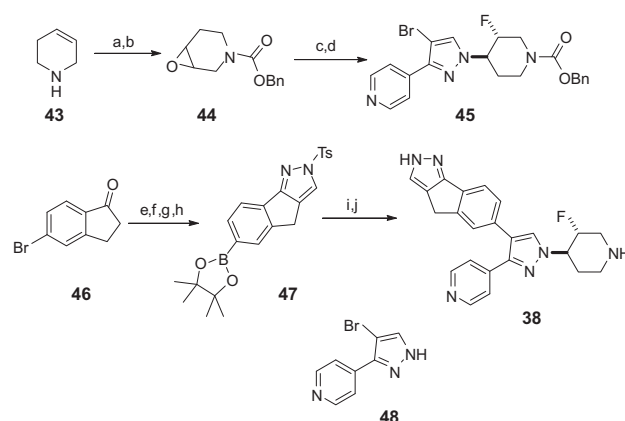
Caco-2 permeability (A–B P_{app} (10^{-6} cm/s) of 1.88, efflux ratio = 6.17), possibly due to the basicity of the piperidine. A series of substituted piperidines were then prepared with the intention of modifying the basicity of the piperidine nitrogen to improve their physicochemical properties, and their oral absorption (Table 3).

Utilizing established techniques to attenuate amine basicity,¹⁴ compounds **36–42** were synthesized. Compounds **37–39**, **41** and **42** essentially had similar cell potencies. No strong enantiomeric (**41** and **42**) or diastereomeric (**38** and **39**) preferences were observed. Hydroxypiperidine **36** showed an approximate sevenfold drop in cell activity relative to its fluoropiperidine counterpart **38**, possibly due to its more basic nature. Fluoropiperidine **40** suffered a similar fate likely due to the nitrogen now being one carbon atom farther away from the fluorine. Caco-2 permeability of compound **38** showed an A–B P_{app} (10^{-6} cm/s) of 11.36 (efflux ratio of 1.55), a significant improvement over compound **26** which had an A–B P_{app} (10^{-6} cm/s) of 1.88 (efflux ratio = 6.17). Similar trends were observed in the oxime series.

We next explored the pharmacokinetic properties of compound **38** (Table 4). CD-1, male mice were dosed (60% PEG400/40% saline solution) 2.5 mg/kg intravenously (iv) and 25, 50, or 100 mg/kg, orally (PO). High clearance was observed (91.1 ml/min/kg) following

Table 4Pharmacokinetics of compound **38** in CD-1 mice

	iv	po	po	po
Dose (mg/kg)	2.5	25	50	100
AUC (μg h/ml)	0.406	5.16	13.4	38.8
CL (ml/min/kg)	91.1	—	—	—
V _{ss} (l/kg)	8.74	—	—	—



Scheme 1. Reagents and conditions: (a) *N*-(benzyloxycarbonyloxy) succinimide, 1:1 dioxane:10% aqueous potassium carbonate (100%); (b) MCPBA, DCM, 0 °C (100%); (c) compound **48**, cesium carbonate, DMSO, 100 °C (30%); (d) DAST, DCM, 0 °C, (37%); (e) DMF–DMA, toluene, Δ (93%); (f) hydrazine, cat. AcOH, EtOH, Δ (22%); (g) NaH, TsCl, THF, 0 °C (70%); (h) bis(pinacolato)diboron, PdCl₂(dppf) DCM adduct, KOAc, dioxane, 100 °C (97%); (i) compound **45**, Pd(PPh₃)₄, potassium carbonate, DME/water, 80 °C then 1 M aqueous NaOH, MeOH, 60 °C (51%); (j) Pd(OH)₂, MeOH, balloon of H₂ (52%).

iv dosing, and a trend toward greater than proportional increases in exposure with increasing dose was observed following oral dosing. It should be noted that compound **38** was 547 nM in a CYP3A4 inhibition assay.

Kinase selectivity was next determined for analog **38**. This compound was screened against a panel of over 200 kinases, and the only significant activity observed was against c-Raf (9% POC at 1 μM).

The synthesis of compound **38** is outlined in Scheme 1. Compound **44** was prepared by Cbz protection of amine **43**, followed by m-CPBA epoxidation gave intermediate **44**. Epoxide ring opening by compound **48**⁶ gave a mixture of regioisomers (attack at the C-4 and C-3 of the epoxide, C4 attack predominating).¹⁵ Subsequent treatment with DAST gave fluoride **45**. It is interesting to note that the product of retention was observed for this fluorination,¹⁶ which was confirmed by ¹H NMR analysis. The desired fused pyrazole coupling partner **47** was prepared from 5-bromoindanone **46** via an enaminoketone intermediate, followed by cyclization, tosylation (one regioisomer) and boronate ester formation. Coupling of **45** and **47** under standard Suzuki conditions followed by de-protection afforded compound **38**. Similar synthetic protocols were used to obtain other oxime replacement analogs.

We have prepared several fused pyrazole B-Raf inhibitors that showed excellent enzyme activity, encouraging cellular potency, and chemical stability over its oxime counterpart. Optimization of the fused pyrazole inhibitor led to fluorine substituted piperidine **38** which showed modest oral absorption in mice and good kinase selectivity. Further progress on these inhibitors will be reported in due course.

Acknowledgment

The authors thank Andrew Allen for NMR analysis and Susan Rhodes, Jennifer Otten, and Michelle Livingston for Caco-2, P450, and solubility determinations.

References and notes

- (a) Hoshino, R.; Chantani, Y.; Yamori, T.; Tsuruo, T.; Oka, H.; Yoshida, O.; Shimada, Y.; Ari-I, S.; Wada, H.; Fujimoto, J.; Kohno, M. *Oncogene* **1999**, *18*, 813–822; (b) Li, N.; Batt, D.; Warmuth, M. *Curr. Opin. Invest. Drugs* **2007**, *8*, 452–456.
- (a) Davies, H.; Bignell, G. R.; Cox, C.; Stephens, P.; Edkins, S.; Clegg, S.; Teague, J.; Woffendin, H.; Garnett, M. J.; Bottomley, W.; Davis, N.; Dicks, E.; Ewing, R.; Floyd, Y.; Gray, K.; Hall, S.; Hawes, R.; Hughes, J.; Kosmidou, V.; Menzies, A.;

- Mould, C.; Parker, A.; Stevens, C.; Watt, S.; Hooper, S.; Wilson, R.; Jayatilake, H.; Gusterson, B. A.; Cooper, C.; Shipley, J.; Hargrave, D.; Pritchard-Jones, K.; Maitland, N.; Chenevix-Trench, G.; Riggins, G. J.; Bigner, D. D.; Palmieri, G.; Cossu, A.; Flanagan, A.; Nicholson, A.; Ho, J. W. C.; Leung, S. Y.; Yuen, S. T.; Weber, B. L.; Seigler, H. F.; Darrow, T. L.; Paterson, H.; Marais, R.; Marshall, C. J.; Wooster, R.; Stratton, M. R.; Futreal, P. A. *Nature* **2002**, 417, 949–954; (b) Cohen, Y.; Xing, M.; Mambo, E.; Guo, Z.; Wu, G.; Trink, B.; Beller, U.; Westra, W. H.; Ladenson, P. W.; Sidransky, D. *J. Natl. Cancer Inst.* **2003**, 95(8), 625–627; (c) Xu, X.; Quiros, R. M.; Gattuso, P.; Ain, K. B.; Prinz, R. A. *Cancer Res.* **2003**, 63(15), 4561–4567.
3. (a) Kalinsky, K.; Haluska, F. G. *Expert Rev. Anticancer Ther.* **2007**, 7, 715–724; (b) Dhillon, D. S.; Hagan, S.; Rath, O.; Kolch, W. *Oncogene* **2007**, 26, 3279–3290.
 4. Wan, P. T.; Garnet, M. J.; Roe, S. M.; Lee, S.; Niculescu-Duvaz, D.; Good, V. M.; Jones, C. M.; Marshall, C. J.; Springer, C. J.; Barford, D.; Marais, R. *Cell* **2004**, 116, 855–867.
 5. McCubrey, J. A.; Milella, M.; Tafuri, A.; Martelli, A. M.; Lunghi, P.; Bonai, A.; Cervello, M.; Lee, J. T.; Steelman, L. S. *Curr. Opin. Invest. Drugs* **2008**, 9, 614–630.
 6. Hansen, J. D.; Grina, J.; Newhouse, B.; Welch, M.; Topalov, G.; Littman, N.; Callejo, M.; Gloor, S.; Martinson, M.; Laird, E.; Brandhuber, B. J.; Vigers, G.; Morales, T.; Woessner, R.; Randolph, N.; Lyssikatos, J.; Olivero, A. *Bioorg. Med. Chem. Lett.* **2008**, 18, 4692–4695.
 7. (a) Choo, E. F.; Driscoll, J. P.; Feng, J.; Liederer, B.; Plise, E.; Randolph, N.; Shin, Y.; Wong, S.; Ran, Y. *Xenobiotica* **2009**, 39(09), 700–709; (b) Coutts, R. T.; Dawe, R.; Dawson, G. W.; Kovach, S. H. *Drug Metab. Disp.* **1976**, 4, 35–39; (c) Heberling, S.; Girreser, U.; Wolf, S.; Clement, B. *Biochem. Pharmacol.* **2006**, 71, 354–365.
 8. PDB accession code 3D4Q.
 9. (a) Tautomer preferences were computed using the 6-31G(d) basis set. Frisch, M. J. et al. *GAUSSIAN98, Revision A.11*, Gaussian: Pittsburgh, PA.; (b) Free energies of solvation were calculated using SM2.1 Amsol 5.0: Cramer, C. J.; Hawkins, G. D.; Lynch, G. C.; Giesen, D. J.; Rossi, I.; Storer, J. W.; Truhlar, D. G.; Liotard, D. A. In *AMSOL-version 5.0, Quantum Chemistry Program Exchange Program 606, based in part on AMPAC-version 2.1*, Liotard, D. A.; Healy, E. F.; Ruiz, J. M.; Dewar, M. J. S.
 10. For assay description see: Laird, E.; Lyssikatos, J.; Welch, M.; Grina, J.; Hansen, J.; Newhouse, B.; Olivero, A.; Topolav, G. WO 2006/084015 A2, 2006.
 11. Computed relative energies for the two pyrazole tautomers indicates a significant population of the undesired tautomer also exists (data not shown).
 12. Ren, L.; Wenglowksy, S.; Miknis, G.; Rast, B.; Buckmelter, A. J.; Ely, R. J.; Schlachter, S.; Laird, E. R.; Randolph, N.; Callejo, M.; Martinson, M.; Galbraith, S.; Brandhuber, B. J.; Vigers, G.; Morales, T.; Voegtli, W.; Lyssikatos, J. *Bioorg. Med. Chem. Lett.* **2011**, 21, 1243–1247.
 13. Tao, Z.-F.; Sowin, T.; Lin, N.-H. *Tetrahedron Lett.* **2005**, 46, 7615–7618.
 14. (a) Hagmann, W. *J. Med. Chem.* **2008**, 51, 4359–4369; (b) Bohm, H.-J.; Banner, D.; Bendels, S.; Kansay, M.; Kuhn, B.; Muller, K.; Obst-Sander, U.; Stahl, M. *ChemBioChem* **2004**, 5, 637–643; (c) van Niel, M. B.; Collins, I.; Beer, M. S.; Broughton, H. B.; Cheng, S. K. F.; Goodacre, S. C.; Heald, A.; Locker, K. L.; MacLeod, A. M.; Morrison, D.; Moyes, C. R.; O'Connor, D.; Pike, A.; Rowley, M.; Russell, M. G. N.; Sohal, B.; Stanton, J. A.; Thomas, S.; Verrier, H.; Watt, A. P.; Castro, J. *J. Med. Chem.* **1999**, 42, 2087–2104.
 15. Determined by ¹H NMR.
 16. Shellhamer, D. F.; Briggs, A. A.; Miller, B. M.; Prince, J. M.; Scott, D. H.; Heasley, V. L. *J. Chem. Soc., Perkin Trans. 2* **1996**, 973–977.